

UNIVERSITÀ DEGLI STUDI DI SIENA
FACOLTÀ DI INGEGNERIA



Corso di Laurea Specialistica in Ingegneria Informatica

*Implementation of the Object Motion-Decoupled
Internal Force Control and evaluation on the
multifingered robotic hand DLR Hand II*

Relatore

Prof. Domenico Prattichizzo

Correlatori

Dipl-Ing. Thomas Wimböck

Dott. Monica Malvezzi

Tesi di laurea di

Marco Aggravi

A. A. 2010/2011

12 Dicembre 2011

Contents

1	Introduction	1
1.1	Introduction	1
1.2	Objectives of the Thesis	3
1.3	Thesis Overview	3
2	Underactuation and Synergies	5
2.1	The Human hand	5
2.2	Robotics hands	6
2.3	Previous studies about Underactuation	7
2.4	Postural Synergies	7
2.5	Synergies contribution to the Thesis	8
3	Robotic Hand Control	9
3.1	An overview on hand models	9
3.1.1	Assumptions and simplifications	9
3.1.2	Hand models	11
3.2	Synergies applied to robotic hand	13
3.2.1	Synergy-Level Impedance Controller	13
3.3	Object Displacement	16
3.3.1	Conditions leading to object displacement	16
3.3.2	Underactuated hands and the problem of controlling both internal forces and object motion	16

3.3.3	Fundamentals of grasping	17
3.3.4	Proposed controller	22
3.3.5	Postural Synergies integration	24
4	Simple Gripper	26
4.1	Physical description of the model	26
4.2	Mathematical description of the model	28
4.3	Additional considerations	30
4.4	Presentation of results	31
5	Evaluations	34
5.1	Simulations	34
5.1.1	Four Fingers Hand Simulator	35
5.1.2	Hand controller integration	41
5.1.3	Postural Synergies control	44
5.1.4	Assumptions	46
5.2	Experiments	47
5.2.1	Hardware for experiments	47
5.2.2	Assumptions	48
5.2.3	Modification to the original model	49
5.2.4	Setup	51
5.2.5	Settings	52
5.2.6	Performance	52
5.3	Problems solved	53
5.4	Problems unsolved	54
5.4.1	Cascaded control loops	55
5.4.2	Quasi-static analysis vs. dynamical simulation	56
5.4.3	Time dependencies	57
5.5	Software used	58

6 Discussion	59
7 Conclusions	63
7.1 Conclusions	63
7.1.1 Future Works	64
Bibliography	66

List of Figures

3.1	References for the fingers and DII Virtual Hand model	12
3.2	DLR Hand II 3D Viewer	12
3.3	Control Flow - Synergy-Level Impedance Controller, from [3] .	15
4.1	Simple Gripper, one axis version	26
4.2	Signal flow chart Simple Gripper	29
4.3	Object displacement with and without compensation	32
4.4	Object Displacement control obtained with equations in Section 3.3 - draft caption	33
5.1	DLR Hand II	35
5.2	DLR Hand II with the object base frame	37
5.3	Plot object displacement, with and without compensation . .	40
5.4	3D Object displacement with and without compensation . . .	41
5.5	Real hand Simulink control model	42
5.6	Control flow Synergies Integration, synergy approach	45
5.7	Control flow Synergies Integration, joint approach	46
5.8	Object Tracking Block	50
5.9	Cascaded control loops	55
6.1	General four fingers model structure	60
6.2	Plot results on the third step	61

List of Tables

4.1	Settings Simple Gripper	32
4.2	Results compensation action on Simple Gripper	32
5.1	Settings Four Fingers	37
5.2	Results compensation action on the Four Fingers model	39
6.1	Results compensation action on the third step	61

Chapter 1

Introduction

1.1 Introduction

Recently, robotics granted a big importance as a support tool for the human. Some areas like industry, surgery medicine, handling of dangerous and toxic materials and physical rehabilitation are examples of this integration between human and machine, with increasing number of application fields. In some of these areas, it is strongly important to have the maximum precision; activities like cutting a human tissue with a scalpel or managing harmful wastes are example that show the entity of the problem.

While obtaining high precision in static cases is easy nowadays, with multiple techniques, holding a certain level of precision during movements of the robotic device is still a problem under analysis. A clarifying example can be found in the movement of a robotic arm during a surgical operation. Let's suppose that the arm, equipped with a robotic hand grasping a scalpel, has to move because the operation on one side is done and has to be done in another part of the tissue; during the motion the hand has to hold the tool, but the gravity and the inertia of the object and of the hand can involve

contact force variations that produce object motion or, in the worst case, the contact loss. It is clear, that in this case the object will not be in the correct position for the next cut.

A way to avoid this problem can be to squeeze the object stronger while moving the arm; however, this action cannot lead to a failure of the grasp, but still to a movement of the grasped object. From the analysis of the rigid-body movements that can be operated on the object, it is possible to find some recovery actions that allow to modify squeezing forces with zero displacement of it.

A good control action of the joints can be achieved using different types of controller. Classical approaches can be controlling position of the joints, with a normal position or a Cartesian controller, or controlling torques/positions of the joints related to the object. Examples of the second case can be found in the Virtual Object approach, that can be divided in force control and impedance control.

In this work, a compliance approach is considered; thinking, and implementing, the mechanical joints as compliant devices permits to use the classical control theory in order to reach good results in terms of robustness and stability.

It is worth to remember that this situation is rare in case when is possible to control all the joint positions (or torques) independently, like in case of fully-actuated hands. When the number of actuated Degrees of Freedom is small, i.e. underactuated case, the problem described above is more frequent. An example of underactuation is those based on the Postural Synergies.

1.2 Objectives of the Thesis

The goal of this work is the study and the implementation of a controller for robotic devices that permits to modify grasping forces avoiding movements of the grasped object.

The idea here analyzed was developed by Domenico Prattichizzo and Monica Malvezzi, of the Department of Information Engineering of the University of Siena, and described in [1].

After a preliminary study phase, the static controller was extended and adapted to work together with the impedance controlled robot hands. Then the controller was implemented and evaluated with simulation and experiments on the robotic device DLR Hand II, developed by the Institute of Robotics and Mechatronics of the German Aerospace Center (DLR), in Oberpfaffenhofen, near Munich.

1.3 Thesis Overview

This work is divided in 7 chapter, including this introduction and a conclusive chapter.

In Chapter 2 the concept of Postural Synergies will be introduced and their use will be explained within robotics, giving also some details about Santello et al. work, following [2].

In Chapter 3 generalizations about human hand will be introduced. In the second part the work of Wimböck et al. on the application of the Postural Synergies concept on the DLR Hand II is described. The final part of the

chapter is instead devoted to the study of the object displacement and of the controller proposed by Prattichizzo et al.

In the Chapter 4 the problem of the object displacement is faced with considering a very simple example, two one-joint-fingers squeezing a mass. On this system, the controller implemented in Simulink, is evaluated with several simulations.

The following steps are shown in the Chapter 5, where the simple model from the Chapter 4 is improved. In this chapter the simulator of the robotic device is shown and the Postural Synergies integration is introduced. In the second part of the chapter is reserved to the experiments: hardware used, assumptions and settings are depicted, and conclusions about the results are given.

In the last part the solved and unsolved problems are discussed.

Chapter 6 contains results of the study, the simulation and the real experiments performed and comments are given.

In Chapter 7 conclusions are given and future works are introduced.

Chapter 2

Underactuation and Synergies

2.1 The Human hand

The human hand is a complex apparatus. It is made of an incredible numbers and varieties of sensors, receptors, neurons, muscles and articulations. This entangled web of mixtures is lead by the human brain, that is well known as the principal source of all the commands given to our body. There exists a theory that the human kind is this way because of his hand, and that is the most powerful tool that he can use. In ancient times, there were many philosophical arguments, like the one between Aristotele and Anaxagoras about the relation between the human hand and the human intelligence.

What is clear, is that the human kind developed during centuries an incredible dexterity with his apparatus and the world as it is now is a consequence and a reflection of this. This explains the great interest of the robotics researchers in reproducing the human hand for helping, and perhaps, supporting the human in difficult or dangerous operations.

Significant progress has been made in studying and replicating the behavior of the human hand, even though many points still remain open; replication

of the human hand in a similar device is very far from the point it started, many years ago, but is far as well from the goal.

2.2 Robotics hands

Several studies were attempt to discover and explain the human complex apparatus. Note on them can be found in [13].

Further details about the kind of assumptions and simplifications that researchers made during this process of replication can be found in Chapter 3. At this point, two ways can be easily highlighted on this replication process: the first is to try to reduce dimensions of the components of the robotic device, to develop a complex and complete sensor skin and to continue the process on the main road, trying to reach the size and the wideness of equipment that the human hand has.

The second way, that is called underactuation, is to try to reduce in particular the number of actuators which the robotic hand is composed, analyzing more in details the control mechanisms and getting inspired by the way the brain commands the hand. The idea is to isolate possible macro-controls that work with the reduced equipment.

The differences between the two approaches can be seen in the fact that for the second approach the size and the weight of the robotic device is reduce but is reduced as swell the possibility to control all the joints indipendently. The two ways are for sure not neglecting each other; they are parallel roads to the same goal and however, also if sometimes they are crossing and sometimes are diverging, it will be difficult to success in the replication process considering only one of these possible ways.

A good merge of the two possibilities is to keep a full equipment hand, with a trustful number of actuators and joints, while using an underactuated approach to the control of that. This is very used nowadays because it doesn't

require to construct new devices and permits to exploit the power of this relative new concept.

In the work presented in this thesis, both ways will be considered, starting from a full actuation system and then switching to the underactuation way.

2.3 Previous studies about Underactuation

The underactuation concept has its fundamentals in the idea that the brain doesn't command all muscles and its joints independently, that there must be a joined way to control and move together sectors of muscles or groups of joints. Finding how to implement this on a robotic hand can open doors in the underactuation fields that permit to advance in the difficult road of the human hand replication.

The concept of a coupled control of the human hand joint interests researcher since centuries; examples can be found in [14], where scientists and academic people were studying the human apparatus in order to discover a coordinated control of it.

A detailed analysis of these studies is made in [14].

2.4 Postural Synergies

In the late 90ies, Santello et al. addressed as well the known problem of the Postural Synergies. They performed a large number of experiments, in which they were asking people to grasp a certain kind of object while tracking joint movements during the (only imagined) manipulation.

The result was a huge database of data representing the joint kinematics during grasp. On this database they performed a PCA analysis in order to find new coordinates for the gestures. The results were 15 different macro-

gestures that they defined Postural Synergies.

They are in fact coupled movements of joints; moving along one synergy direction is like moving along a coupling space that is defined by that synergy. This is in fact the imagined connection between coordinated commands sent by the brain and the movements of the hand.

From this analysis, a relation between hand joint positions and these macro-gestures can be found. Defining $\mathbf{q}(t)$ the hand joints vector, composed by the joints angles at a certain instant of time, $\mathbf{z}(t)$ the synergies vector at the same instant and \mathbf{S} the Synergy Matrix, is possible to define the relation between these two vector as following

$$\mathbf{q}(t) = \mathbf{S}\mathbf{z}(t). \quad (2.1)$$

This equation can be extended also to the differential approach, with $\delta\mathbf{q}(t) = \mathbf{S}\delta\mathbf{z}$.

Further details about the analysis that leads to the Postural Synergies can be found in [2].

2.5 Synergies contribution to the Thesis

As said before, and as will be point out again in the following chapter, having a smaller possibility to control the joints independently can lead more often to a displacement of the object while changing internal forces, with respect of the fully-actuated approach. The concept of the Postural Synergies is considered in this work because there is the necessity to threat the robotic device has underactuated system, even if the manipulator is fully-actuated, like in the case of the DLR Hand II.

Chapter 3

Robotic Hand Control

3.1 An overview on hand models

3.1.1 Assumptions and simplifications

A human hand is a very complex system, with integration of sensors, neuroreceptors, actuators, all merged together in an organic form that is still not well known. For this reason, when the purpose is the realization of anthropomorphic robotic hand, researchers and constructors make assumptions and simplifications in order to speed up this process and to compensate the not-perfect knowledge of our complex appendix.

Simplifications made during the transition between human hands and robotic hands are usually at the level of joints, in the equipment of sensors and in the kind of commands that are given to the robotic system.

At the state of art it is not possible to replicate human muscles and organic systems like in the real apparatus. Designers typically model the human joints with rotational joints, that are moved with motors or tendons.

In the first case the joint itself is provided with a motor and the amount

of needed current is given as command. In this approach the controller has to calculate is the amount of power that has to be given in order to reach the desired position or the desired motor torque.

In the second case, the joints act like pulleys and are moved by tendons which are stretched from motors positioned usually in the hand base. In this type of modeling the angular position of the joints depend on how much the tendons are stretched, i.e. a slightly more complicated control has to be done to command a desired position or a desired torque of the joint.

The first method requires simpler controller but the mechanics lie in the hand, that increase the total weight of that.

In the second approach, this is avoided, considering that all the motors are moved to the forearm, but the control action needed is more complex. In addition, the second method requires more constant maintenance and high quality wires for the tendons are necessary.

Example of the two different types of actuations can be found in the DLR Hand II, [4], for the first case, and in the hand mounted on the DLR Hand-Arm-System, [18], for the second.

Another big difference between robotic hands and human ones is the sensor equipment. The human skin is a thin and very complex web of sensors and at the state of art nothing can be comparable to that, in term of efficiency and dimension. To bypass this problem, robotic hands are usually equipped with a great range of sensors; typically torque sensors on joints¹, temperature sensors and force sensors are integrated.

However, tough this way is useful to solve a wide range of problems related to

¹It is worth to remember that very few robotic hands nowadays are provided of joint torque sensing.

measurements needed during grasp activity, it is not enough. Complex sensor systems, like artificial skins, are under study; an example can be found in the IIT artificial skin for iCub [5]. Anyway, this remains an open field and once it will be covered enough will give a strong push in the understanding of the complex human interaction between sensor system and control system.

A complete understanding of how our brain commands the hands is far to be achieved. Detailed studies were made and a certain level of knowledge on how this complex process works was reached. However, yet a lot of analysis on the physical and neuronal mechanisms and integrations is needed.² To get around this problem, a classical approach is to command directly how joints must move in order to reach an objective. Typically this objective can be a certain positions of the fingertip, a certain torque applied from the hand to an object, or a certain grasp of an object. One innovative way of thinking about how to command (or how the brain commands) the hand is based on the concept of the Postural Synergies, already introduced in the Chapter 2.

3.1.2 Hand models

A very good example of how to model the human hand in a virtual environment can be found in [6], where the authors performed a in-depth analysis of the human hand structure in order to replicate realistically the kinematics and the dynamics of the human appendix. The resulting model is shown in Fig 3.1.

For the robotic device used in the experiments, the Institute is provided with a 3D Viewer of the hand, that is reproducing trustfully the device. A screen of this software can be seen in Fig 3.2.

²Related works can be found in <http://www.thehandembodied.eu/papers>.

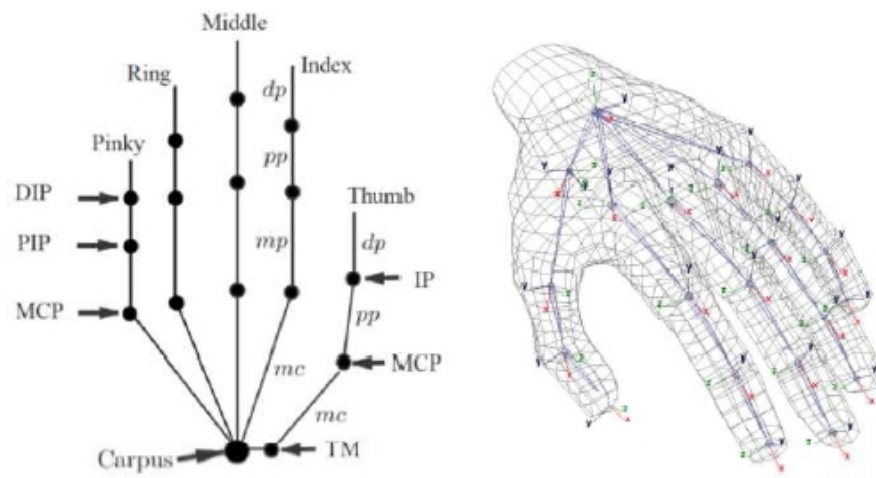


Figure 3.1: References for the fingers and DII Virtual Hand model

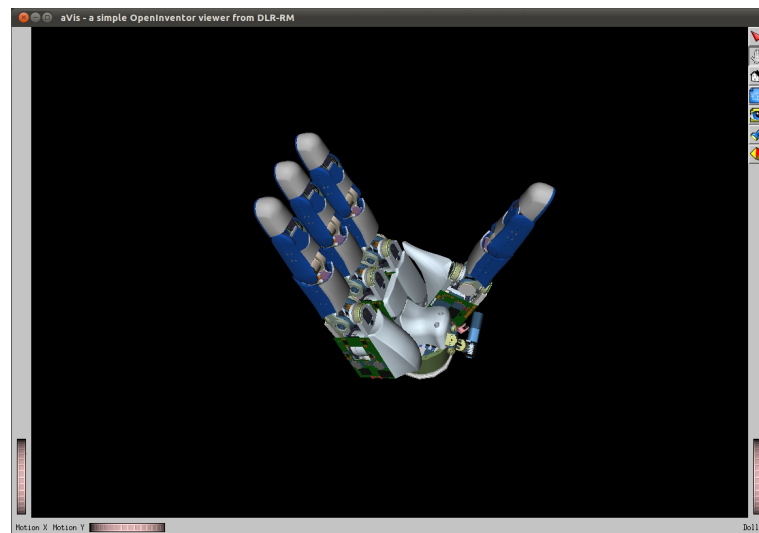


Figure 3.2: DLR Hand II 3D Viewer

3.2 Synergies applied to robotic hand

The work of Wimböck et al. [3] related to the use of postural synergies in the control of an anthropomorphic hand like the DLR Hand II is described in this section. The results of this work are integrated in the simulator implementing the proposed controller.

3.2.1 Synergy-Level Impedance Controller

Studies related to the postural synergies inspired several ideas about reducing the control space of robotic hands and about underactuation. The idea of Wimböck et. al was to reproduce a similar analysis about postural synergies to the anthropomorphic DLR Hand II. From this approach twelve synergy-like couplings were found and Synergy based controller were implemented.

During years the institute of RM collected a huge amount of grasping data performed with the DLR Hand II device. This database contained several types of grasping and gestures; the authors rearranged the dataset excluding biases from mean values and they isolated 26 most reasonable grasp postures. On this reduced dataset a Principal Component Analysis was performed and they were able to isolate few principal components representing the so-called postural synergies for the specific device. In fact, they were able to discover up to 3 synergy coordinates, while other degrees of freedom were used to represent the underactuation. It is worth to note that the study of Santello on the postural synergies is strongly related to the human hand and to how is made and composed. Considering this, what the authors found here is not a subset of the postural synergies of Santello; they were indeed able to circumvent the problem of how to map human data to a robotic device and to define a specific set of synergies, valid only for the DLR Hand II.

The analysis of the principal components revealed that with two synergies

a range of 74% of grasps were reached and they considered this threshold enough for an appropriate approximation by the synergies.

Defining the robot hand configuration as

$$\mathbf{q} = (q_1 \dots q_{n_q})^T \in \mathbb{R}^{n_q}$$

and $\bar{\mathbf{q}}$ as the mean joint configuration, the authors depicted the relation between the joints variables and the postural synergies as

$$\mathbf{q} = \mathbf{S}\mathbf{z} + \bar{\mathbf{q}} \quad (3.1)$$

where $\mathbf{S} \in \mathbb{R}^{n_q \times n_z}$ is the synergy matrix, with n_z number of synergies taken in account. It is worth to remember that $n_z \ll n_q$.

Considering the dynamics in the hand joints space as is written in [7]

$$\mathbf{M}(\mathbf{q})\ddot{\mathbf{q}} + \mathbf{C}(\mathbf{q}, \dot{\mathbf{q}})\dot{\mathbf{q}} + \mathbf{g}(\mathbf{q}) = \boldsymbol{\tau} + \boldsymbol{\tau}_{ext} \quad (3.2)$$

they rewrote (3.2) in the synergy space as

$$\boldsymbol{\Lambda}(\mathbf{q})\ddot{\mathbf{z}} + \boldsymbol{\mu}(\mathbf{q}, \dot{\mathbf{z}})\dot{\mathbf{z}} + \mathbf{F}_g(\mathbf{q}) = \boldsymbol{\eta} + \boldsymbol{\eta}_{ext} \quad (3.3)$$

The inertia matrix, the Coriolis and centrifugal matrix, the gravity forces and the input forces with respect to the the synergy coordinates are:

$$\begin{aligned} \boldsymbol{\Lambda}(\mathbf{q}) &= \mathbf{S}^T \mathbf{M}(\mathbf{q}) \mathbf{S}, \\ \boldsymbol{\mu}(\mathbf{q}, \dot{\mathbf{q}}) &= \mathbf{S}^T \mathbf{C}(\mathbf{q}, \dot{\mathbf{q}}) \mathbf{S}, \\ \mathbf{F}_g(\mathbf{q}) &= \mathbf{S}^T \mathbf{g}(\mathbf{q}), \\ \boldsymbol{\eta} &= \mathbf{S}^T \boldsymbol{\tau}. \end{aligned}$$

From this mathematical base, the synergy based impedance controller proposed is based on a desired impedance behavior like

$$\boldsymbol{\Lambda}_d \ddot{\mathbf{e}}_z + \mathbf{D}_d \dot{\mathbf{e}}_z + \mathbf{K}_d \mathbf{e}_z = \boldsymbol{\eta}_{ext} \quad (3.4)$$

where $\mathbf{e}_z = (\mathbf{z} - \mathbf{z}_d)$ is the deviation of \mathbf{z} to a desired virtual equilibrium position \mathbf{z}_d . The matrices of the desired inertia $\mathbf{\Lambda}_d \in \mathbb{R}^{n_z \times n_z}$, damping $\mathbf{D}_d \in \mathbb{R}^{n_z \times n_z}$ and stiffness $\mathbf{K}_d \in \mathbb{R}^{n_z \times n_z}$ are symmetric and positive definite. The control law of the controller is

$$\eta = \mathbf{\Lambda}(\mathbf{q})\ddot{\mathbf{z}}_d - \mathbf{D}_d\dot{\mathbf{e}}_z - \mathbf{K}_d\mathbf{e}_z \quad (3.5)$$

$$\tau_c = \mathbf{g}(\mathbf{q}) + \mathbf{S}\eta \quad (3.6)$$

that also ensures the gravity compensation. Hence the controller deals only with n_z synergies, there is a large nullspace that has to be managed. The authors made this including in the controller a similar impedance contribution

$$\tau_n = -\mathbf{D}_n(\dot{\mathbf{q}}) - \mathbf{K}_n(\mathbf{q} - \dot{\mathbf{q}}) \quad (3.7)$$

and with the possibility to set independently stiffness and damping respectively for the synergy part and for the nullspace part. Projecting (3.7) in the nullspace of \mathbf{S}^T and inserting that in (3.6), they obtained the following control law ³

$$\tau = \mathbf{g}(\mathbf{q}) + \mathbf{S}\eta + (\mathbf{I} - \mathbf{S}\mathbf{S}_{M-1}^+) \tau_n$$

Here is shown the control flow of the controller proposed in [3] and in the box is shown the artificial kinematic coupling.

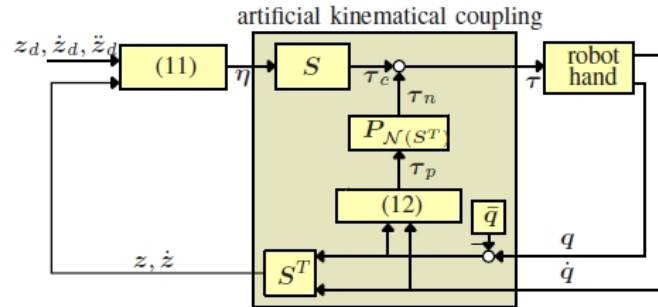


Figure 3.3: Control Flow - Synergy-Level Impedance Controller, from [3]

³Notes about projection in the [3].

3.3 Object Displacement

3.3.1 Conditions leading to object displacement

Internal forces are a fundamental part of the theory of grasping and controlling them in a correct way is necessary in most of the manipulation and grasp tasks. In fields like surgery or industry is necessary a very good precision in the manipulation of the object (like with scalpel or with corrosive liquids or human lethal materials).

In these tasks, a decoupled object motion and internal force control is needed. Consider a compliant implementation and the possibility to cannot control all the joints independently. In this case, it is possible that the object moves when the internal forces are varied.

3.3.2 Underactuated hands and the problem of controlling both internal forces and object motion

When a fully-actuated approach is considered, the object displacement is avoidable because is possible to control all the internal forces and object motions.

If this approach is not anymore taken in account but the possibility to control the joints independently is reduced the dimensions of controllable internal forces and object motions decrease. Further details can be found in [15].

It is possible to divide the second situation in two parts: having an actual underactuated device which input are reduced or having a fully-actuated device which input are calculate using an underactuation notion.

In the first approach, what must be done is to calculate the input for the device using a *underactuated controller* (like the proposed controller with

the inclusion of the Postural Synergies), i.e. having a controller that gives directly the reduced input for the device.

In the second approach instead is to calculate references for the device in the full-actuated joint space and then to *map* this input in the correct space for the underactuation.

In other words, in the first approach the reduction of the input is made inside the controller while in the second approach is done within the device.

3.3.3 Fundamentals of grasping

Here some fundamentals of grasping are depicted. From them, an analysis of the conditions leading to object displacement is made and one possible control of that is proposed.

For all the followings more details can be found in [8].

Considering a robotic device grasping an object two coordinates frame are defined, one for the device base $\{\mathbf{N}\}$ and one related to the object $\{\mathbf{B}\}$.

Taking $\{\mathbf{N}\}$ as the reference system, $\{\mathbf{B}\}$ is the body frame and the translational distance between the two frames is represented by \mathbf{p} while the relative rotation between the two systems is ϕ . With this notation the position of the object \mathbf{u} is defined as $\{\mathbf{p}, \phi\}^T \in \mathbb{R}^{6 \times 1}$. The twist of the object ν_u , that represents the generalized velocity of the object with the respect of $\{\mathbf{N}\}$, is $\{\dot{\mathbf{p}}, \omega\}^T \in \mathbb{R}^{6 \times 1}$. In the same way, the wrench of the object \mathbf{w} , composed from the generalized forces acting on that, is defined as $\{\mathbf{f}_u, \mathbf{m}_u\}^T$, with \mathbf{f}_u vector of external forces and \mathbf{m}_u moment of the body.

The positions of the device joints are defined as

$$\mathbf{q} = (q_1 \dots q_{n_q})^T \in \mathbb{R}^{n_q}$$

while $\{c_i\}$ is the i -th contact frame. The number of contact points is n_c and the number of the joints is n_q .

With this notation, the velocities of the contact points with respect to the object (ν_c) and to the hand (ν_h) can be defined as

$$\nu_c = \mathbf{G}^T \nu_u \quad \nu_h = \mathbf{J} \dot{\mathbf{q}} \quad (3.8)$$

where $\mathbf{G} \in \mathbb{R}^{6 \times 6n_c}$ is the Grasp matrix, $\mathbf{J} \in \mathbb{R}^{6n_c \times n_q}$ is the hand Jacobian of the manipulator and $\dot{\mathbf{q}} \in \mathbb{R}^{n_q \times 1}$ are the generalized velocities of the joints (n_c number of contact points).

Taking in account the HF contact model (refer to [8] for details) reduces the columns of \mathbf{G} and the rows of \mathbf{J} .

In particular, \mathbf{G} will be in $\mathbb{R}^{6 \times 3n_c}$ and \mathbf{J} will be in $\mathbb{R}^{3n_c \times n_q}$

To satisfy the contact for each instant of time, a constraint on the contact point velocities has to be introduced

$$\mathbf{J} \dot{\mathbf{q}} - \mathbf{G}^T \nu_u = 0 \quad (3.9)$$

Considering the initial position of the contact points on the hand and on the object to be the same, fixing the velocities to an equal value forces the points to not move during all the manipulation task.

Each finger apply a contact force to the object and the sum of all of them can contribute at the changing of the wrench of this one.

In order to reach the static equilibrium for the object the following equation

as to be satisfied

$$\mathbf{G}\lambda_{\mathbf{c}} = -\mathbf{w} \quad (3.10)$$

$\lambda_{\mathbf{c}}$ is the vector of the contact forces and belong to \mathbb{R}^{6n_c} . Considering HF as the contact model, $\lambda_{\mathbf{c}}$ will be in \mathbb{R}^{3n_c} .

From this equation is clear that the forces in the range of $\lambda_{\mathbf{c}}$ belonging to the $\mathcal{N}(\mathbf{G})$ are not contributing to the wrench applied to the object. These forces are called internal forces.

The contact forces on the hand are balanced by the joint torques, according to the following equilibrium equation

$$\tau = \mathbf{J}^T \lambda_{\mathbf{c}}, \quad \tau \in \mathbb{R}^{n_q} \quad (3.11)$$

The contact forces are mapped, via the hand Jacobian, to the joints in the form of torques (or translational forces in case of prismatic joints).

Relaxing (3.9) permits to introduce a mathematical definition of the contact forces that includes contact stiffness. Inserting a spring between each contact point on the object and the one on the fingertip permits to link the magnitude of the contact force, related to this point, to the length of the spring.

The following equation shows how this concept is introduced

$$\delta\lambda_{\mathbf{c}} = \mathbf{K}_c(\delta c^h - \delta c^o) \quad (3.12)$$

Note: It is clear that the number of rows of \mathbf{K}_c determines the dimension of $\lambda_{\mathbf{c}}$; this dimension is indicated with n_{fc} and is equal to $n_c \times j$, where n_c is the number of contact points and j ($j = 3, \dots, 6$) is the dimension of each single contact forces (that depends on the contact model).

From a starting initial equilibrium configuration, it is possible to write variations of contact forces (3.12), in term of compliance and using (3.8), as

$$\mathbf{C}_s \delta \lambda_{\mathbf{c}} = (\mathbf{J} \delta \mathbf{q} - \mathbf{G}^T \delta \mathbf{u}) \quad (3.13)$$

Consider the hand joints controlled in position with their torques proportional to a static gain stiffness \mathbf{K}_q , Eq. (3.13) can be rewritten as

$$\delta \lambda_{\mathbf{c}} = \mathbf{K} (\mathbf{J}_r \delta \mathbf{q}_r - \mathbf{G}^T \delta \mathbf{u}) \quad (3.14)$$

where the total stiffness matrix, taking into account joint and contact compliance, and geometric effects due to the variation of Jacobian matrix, is given by⁴

$$\mathbf{K} = (\mathbf{C}_s + \mathbf{J}_r \mathbf{C}_q \mathbf{J}^T)^{-1} \quad (3.15)$$

$$\mathbf{J}_r = \mathbf{J} (\mathbf{I} + \mathbf{C}_q \mathbf{T}). \quad (3.16)$$

By differentiating eq. (3.10), considering a constant external load, and inserting that in (3.14), results that the object motion δu as a function of the joint reference variation δq_r is

$$\delta \mathbf{u} = \mathbf{V} \delta \mathbf{q}_r \quad (3.17)$$

and the corresponding contact force variation is

$$\delta \lambda_{\mathbf{c}} = \mathbf{P} \delta \mathbf{q}_r \quad (3.18)$$

where

$$\mathbf{V} = (\mathbf{G} \mathbf{K} \mathbf{G}^T + \mathbf{N})^{-1} \mathbf{G} \mathbf{K} \mathbf{J}_r$$

$$\mathbf{P} = (\mathbf{I} - \mathbf{K} \mathbf{G}^T (\mathbf{G} \mathbf{K} \mathbf{G}^T + \mathbf{N})^{-1} \mathbf{G}) \mathbf{K} \mathbf{J}_r$$

⁴see [1] for details

Defining $\mathbf{E} \in \mathbb{R}^{n_{fc} \times e}$ a basis matrix of the column space of \mathbf{P} , is possible to express the generic controllable internal forces as

$$\delta \lambda_{\mathbf{c}} = \mathbf{E} \mathbf{y}$$

where $\mathbf{y} \in \mathbb{R}^e$ is the generic vector that parametrizes the reachable contact forces.

One of the focus point exploited in the controller proposed later can be found in the rigid-body kinematics. The rigid-body motions are the easiest way to move the object. They do not involve virtual contact spring deformation, so they don't change the values of the internal forces. If the control of the internal forces is made considering joint actuations and a movement occurs, is possible to use rigid-body motions to recover it. Rigid-body kinematics has been studied, in quasi-static setting, in term of unobservable subspaces from contact forces and in presence of passive joints.

To find rigid-body kinematics related to a specific system, the solution of the equation (3.9) has to be analyzed.

Let Γ be a matrix that describes rigid kinematics, it is defined as the matrix whose columns form the basis for the nullspace of $[\mathbf{J}_r - \mathbf{G}^T]$. Eq. (3.9) can be rewritten as

$$[\mathbf{J}_r - \mathbf{G}^T] \begin{bmatrix} \delta \mathbf{q}_r \\ \delta \mathbf{u} \end{bmatrix} = 0 \quad (3.19)$$

and the generic solution of (3.19) can be expressed as

$$\begin{bmatrix} \delta \mathbf{q}_r \\ \delta \mathbf{u} \end{bmatrix} = \Gamma x \quad (3.20)$$

It is possible to express Γ as

$$\Gamma = \begin{bmatrix} \Gamma_r & \Gamma_{qc} & 0 \\ 0 & \Gamma_{uc} & \Gamma_i \end{bmatrix} \quad (3.21)$$

where Γ_r is a basis matrix of the subspace of the nullspace of \mathbf{J}_r defining the redundant manipulator motions, Γ_i a basis matrix of the subspace of the nullspace of \mathbf{G}^T defining the indeterminate object motions (not dependent from the manipulator) and Γ_{qc} and Γ_{uc} binds the object motions to the joint movements. The last two are conformal partitions of a complementary basis matrix. Where Γ_i and Γ_r are trivial, the manipulator is not redundant neither indeterminate. This means there are no joints movements that are not moving the object neither object movements that don't have effects on the joints. The column composed by $[\Gamma_{qc} \ \Gamma_{uc}]^T$ define the space of the coordinated rigid-body motions of the mechanism.

As it has been shown in [9, 10, 11] the rigid-body motions are reachable and belongs to the space of reachability of linear system that represents the dynamics of the system.

3.3.4 Proposed controller

Based on the previous section, a generic rigid-body motion, $\delta \mathbf{u}_{rb} = \Gamma_{uc} \beta$, can be defined.

Following the eq. (3.17), the corresponding set of joint displacement can be written as

$$\delta \mathbf{q}_{rb} = \mathbf{V}^\# \delta \mathbf{u}_{rb} + \mathbf{Q} \mathbf{x},$$

where $\mathbf{V}^\#$ is the pseudoinverse of \mathbf{V} , \mathbf{Q} is a matrix composed by columns that form a basis for the nullspace of \mathbf{V} and \mathbf{x} is an arbitrary vector of the same size of the columns of \mathbf{Q} . Considering eq. (3.18), is possible to find the

corresponding internal force variation

$$\delta\lambda_c = \mathbf{P}\mathbf{V}^\# \delta\mathbf{u}_{rb} + \mathbf{P}\mathbf{Q}\mathbf{x}.$$

Now a subspace of internal forces can be defined: an internal force $\delta\lambda_c$ is controllable and compensable if it respects the following properties:

- it can be expressed as $\delta\lambda_c = \mathbf{P}\delta\mathbf{q}_r$, thus is realizable with an action on joints;
- the corresponding object displacement $\delta\mathbf{u}_c = \mathbf{V}\delta\mathbf{q}_c$ belongs to the rigid-body motion subspace and can be recovered with a proper control action.

Considering an arbitrary internal force variation $\delta\lambda_c$. Following (3.18), the contribution on the joints given by this force is

$$\delta\mathbf{q}_f = \mathbf{P}^\# \delta\lambda_c. \quad (3.22)$$

If this force belongs to the subspace of controllable and compensable internal forces, it is possible to find a compensating action that recover the eventual displacement given by (3.22). This action is defined as

$$\delta\mathbf{q}_m = -\Gamma_{qc} \Gamma_{uc}^\# V \delta\mathbf{q}_f. \quad (3.23)$$

The proposed controller is the sum of both contribution, the internal forces control plus the recover action:

$$\delta\mathbf{q}_c = \delta\mathbf{q}_m + \delta\mathbf{q}_f. \quad (3.24)$$

This strategy allows to control internal forces with zero displacement of the grasped object.

As will be point out in the next chapters, here two control modes can be highlighted:

- internal forces control **without** the compensation action, considering only $\delta\mathbf{q}_f$.
- internal forces control **with** the compensation action, considering $\delta\mathbf{q}_f$ and the recover contribution $\delta\mathbf{q}_m$.

3.3.5 Postural Synergies integration

If the number of actuated degrees of freedom is sufficiently high, for example in a fully actuated anthropomorphic hand, it is possible to control all the internal forces without having displacement in the object position. However, while considering underactuation, this space is reduced, thus also the possibility to avoid displacements. This explain why the proposed controller has a primary importance when using an underactuation joint control system.

The proposed controller is tested on simulations performed considering a Postural Synergies approach, as is done in this work. The authors showed how, considering only translational displacement of the simulated object, 4 synergies were sufficient to recover the movement caused by a variation of internal forces along one direction.

The assumption taken in account to switch the joint control space between the complete space to the synergies space is the to considered the following relation

$$\delta\mathbf{q}_r = \mathbf{S}\delta\mathbf{z}$$

where $\delta\mathbf{z} \in \mathbb{R}^{n_z}$ is the variation of the reduced set of inputs and $\mathbf{S} \in \mathbb{R}^{n_q \times n_z}$ is the so-called *synergy matrix*, that maps the input variables \mathbf{z} in the joint space \mathbf{q} .

To use the proposed controller with the reduced control space, the fol-

lowing equation has to be used

$$\mathbf{J}_s = \mathbf{J}\mathbf{S}. \quad (3.25)$$

With this modification, V and P will be

$$\mathbf{V}_s = \mathbf{V}\mathbf{S}, \quad \mathbf{P}_s = \mathbf{P}\mathbf{S}.$$

Considering the contribution of the Postural Synergies modify the control law expressed by the eq. (3.24) as following

$$\delta\mathbf{z}_c = \delta\mathbf{z}_m + \delta\mathbf{z}_f$$

while

$$\delta\mathbf{z}_f = \mathbf{P}_s^\# \delta\lambda_c, \quad \delta\mathbf{z}_m = -\Gamma_{qc}^S (\Gamma_{uc}^S)^\# V_S \delta\mathbf{z}_f.$$

In the section 3.2.1 is shown how the authors designed a controller for the robotic device DLR Hand II exploiting the Postural Synergies concept.

In the Chapter 5 is shown how the two controller can be merged.

Chapter 4

Simple Gripper

The Object Displacement Controller (ODC) was proposed in Chapter 3 and its mathematical fundamentals were described. In the following section one of the simplest case is considered in order to evaluate the control performance. This case is called Simple Gripper and is composed of two fingers with two contact points grasping an object.

4.1 Physical description of the model

The Simple Gripper is composed of two fingers grasping an object. Each finger is modeled as a spring-mass-damper system (SMD) and is in contact with the object. This is implemented with a mass that connects the two fingers.

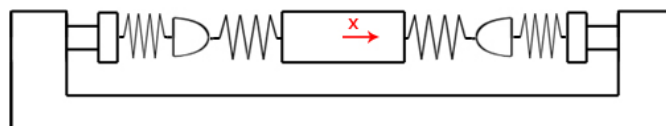


Figure 4.1: Simple Gripper, one axis version

The contact between a fingertip and the object is simulated as another spring-mass-damper system and lies on a single coordinate. Here, the mass of the fingertip is the fix reference while the mass of each finger simulates the fingertip's mass.

The whole system, merging four SMD systems (two contacts and two fingers), has the base frame in the reference position of the object; this frame is 1-D, lying only in the X-axis. For this reason, all the equations representing the system (given below) are composed only by scalar values.

The controlled inputs are the reference values for the fingertips positions. In addition, there are others parameters that can be changed: stiffness and damping of the contact springs, stiffness and damping of the joint springs, virtual masses of the fingertips, initial positions of the fingertips, matrices J and G (following equations in 3.3.3), and commanded internal forces parametrization vector (\mathbf{y}). Time settings, like simulation time and interpolator time in the model don't influence the behavior of the simulation. This is not happening in this case, hence is not considered as a 'real' input. With interpolator time is denote how much the input signal needs in order to reach the final value starting from an initial one (usually 0). Hence in this case the signal is not influenced by the interpolator time, this is not considered as a 'real' input.

Note: In the theory of the ODC we considered rigid body motions, so is necessary that the object is simulated as rigid. In the simulated tests, contact stiffness of around 10^3 higher than the joint ones are used. This comes from the analysis of the mapping of the joints stiffness onto contact. Satisfy this condition is not always possible, following the problem depicted in Section 5.4; for this particular example, with two fingers squeezing an object that was not a problem and between contacts stiffness \mathbf{K}_c and joints stiffness \mathbf{K}_q a ratio of 0.5:1500 (1:3000) is obtained.

4.2 Mathematical description of the model

The mathematical model of the simulated system is described in this paragraph. Considering the well-known SMD equations, the Simple Gripper model is described with the following system

$$\begin{cases} \mathbf{m}_1 \ddot{\mathbf{p}}_{f1} + \mathbf{K}_{c1}(\mathbf{p}_{f1} - \mathbf{u}) + \mathbf{D}_{c1}(\dot{\mathbf{p}}_{f1} - \dot{\mathbf{u}}) = \mathbf{K}_{q1}(\mathbf{x}_{d1} - \mathbf{p}_{f1}) + \mathbf{D}_{q1}(\dot{\mathbf{x}}_{d1} - \dot{\mathbf{p}}_{f1}) \\ \mathbf{m}_2 \ddot{\mathbf{p}}_{f2} + \mathbf{K}_{c2}(\mathbf{p}_{f2} - \mathbf{u}) + \mathbf{D}_{c2}(\dot{\mathbf{p}}_{f2} - \dot{\mathbf{u}}) = \mathbf{K}_{q2}(\mathbf{x}_{d2} - \mathbf{p}_{f2}) + \mathbf{D}_{q2}(\dot{\mathbf{x}}_{d2} - \dot{\mathbf{p}}_{f2}) \\ \mathbf{m}_o \ddot{\mathbf{u}} - \mathbf{K}_{c1}(\mathbf{p}_{f1} - \mathbf{u}) - \mathbf{K}_{c2}(\mathbf{p}_{f2} - \mathbf{u}) - \mathbf{D}_{c1}(\dot{\mathbf{p}}_{f1} - \dot{\mathbf{u}}) - \mathbf{D}_{c2}(\dot{\mathbf{p}}_{f2} - \dot{\mathbf{u}}) = 0 \end{cases}, \quad (4.1)$$

where the state of the system is $\mathbf{x} = [\mathbf{p}_{f1} \ \mathbf{p}_{f2} \ \mathbf{u}]^T \in \mathbf{R}^{n_q}$.

Isolating that in 4.1 and using a stacked notation, the system can be rewritten as

$$\mathbf{M}\ddot{\mathbf{x}} + \mathbf{K}\mathbf{x} + \mathbf{D}\dot{\mathbf{x}} = \mathbf{K}_z \mathbf{z} + \mathbf{D}_z \dot{\mathbf{z}} \quad (4.2)$$

where

$$\begin{aligned} \mathbf{M} &= \begin{bmatrix} \mathbf{m}_1 & 0 & 0 \\ 0 & \mathbf{m}_2 & 0 \\ 0 & 0 & \mathbf{m}_o \end{bmatrix}, \quad \mathbf{D} = \begin{bmatrix} \mathbf{D}_{c1} + \mathbf{D}_{q1} & 0 & -\mathbf{D}_{c1} \\ 0 & \mathbf{D}_{c2} + \mathbf{D}_{q2} & -\mathbf{D}_{c2} \\ -\mathbf{D}_{c1} & -\mathbf{D}_{c2} & \mathbf{D}_{c1} + \mathbf{D}_{c2} \end{bmatrix}, \\ \mathbf{K}_z &= \begin{bmatrix} \mathbf{K}_{q1} & 0 & 0 \\ 0 & \mathbf{K}_{q2} & 0 \\ 0 & 0 & 0 \end{bmatrix}, \quad \mathbf{K} = \begin{bmatrix} \mathbf{K}_{c1} + \mathbf{K}_{q1} & 0 & -\mathbf{K}_{c1} \\ 0 & \mathbf{K}_{c2} + \mathbf{K}_{q2} & -\mathbf{K}_{c2} \\ -\mathbf{K}_{c1} & -\mathbf{K}_{c2} & \mathbf{K}_{c1} + \mathbf{K}_{c2} \end{bmatrix}, \\ \mathbf{D}_z &= \begin{bmatrix} \mathbf{D}_{q1} & 0 & 0 \\ 0 & \mathbf{D}_{q2} & 0 \\ 0 & 0 & 0 \end{bmatrix}. \end{aligned}$$

The contact forces can be defined as

$$\lambda_{ci} = \mathbf{K}_{ci}(\mathbf{p}_{fi} - \mathbf{u}), \quad i = 1, 2$$

and 4.1 becomes

$$\mathbf{M}\ddot{\mathbf{x}} + \Lambda + \tilde{\mathbf{K}}\dot{\mathbf{x}} + \tilde{\mathbf{D}}\dot{\mathbf{x}} = \mathbf{K}_z\mathbf{z}_d + \mathbf{D}_z\dot{\mathbf{z}} \quad , \quad \Lambda = \begin{bmatrix} \lambda_{c1} & 0 & 0 \\ 0 & \lambda_{c2} & 0 \\ 0 & 0 & -\lambda_{c1} - \lambda_{c2} \end{bmatrix} \quad (4.3)$$

that is the equation used to simulate the dynamics of the Simple Gripper model in Simulink.

The control model of the Simple Gripper can be drawn as the following

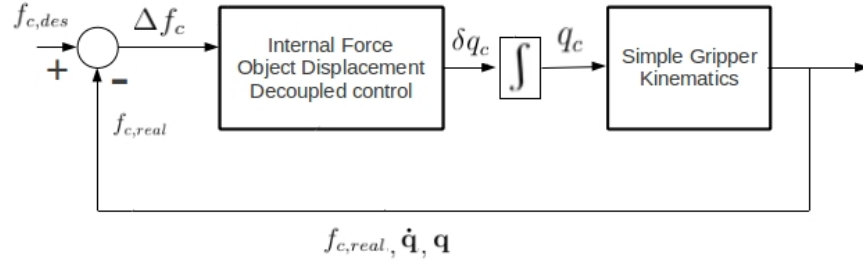


Figure 4.2: Signal flow chart Simple Gripper

where the left hand side block represents the object displacement control law presented in 3.3.

Considering $n_c = 2$, number of contact points, and $n_q = 2$, number of joints, we have that the grasp matrix G belongs to $\mathbf{R}^{1 \times 2}$ and the Jacobian J belongs to $\mathbf{R}^{2 \times 2}$.

Note: The $\delta\lambda$ in the equation is not the same Δf_c in the control flow, resulting from $f_{c,des} - f_{c,real}$. This operations is a mathematical implementation inside Simulink, because is not possible to consider as input infinitesimal dif-

ferences from an equilibrium point. More considerations about this problem are treated in Section 5.4.

4.3 Additional considerations

Consider a spring in the rest condition, i.e. is not stretched or compressed. It has a length that is a property of that particular spring and is depending on its stiffness. This length is called *rest length*, and when considered gives the possibility to limit the compression of the spring as introduces a minimal elongation of that. To insert this concept in the previous equations Λ has to be modified like the following

$$\Lambda_l = \begin{bmatrix} f_{c1} - l_1 & 0 & 0 \\ 0 & f_{c2} - l_2 & 0 \\ 0 & 0 & -f_{c1} - f_{c2} + l_1 + l_2 \end{bmatrix}$$

The resulting forces introduced are called in this work *rest length forces* and are defined as $\Lambda_{li} = K_{ci}l_i$, $i = 1, 2$.

The system described by 4.3 has for steady state solution $f_{c1} = f_{c2}$, for every magnitude of f_{ci} depending on the parameters of the system. This represents a perfect equilibrium between the contact forces, constrained from the third equation (related to the central mass). Change this symmetry between the fingertips and the object is possible using $\Lambda_{l1} = \mathbf{K}_{c1}l_1$ and $\Lambda_{l2} = \mathbf{K}_{c2}l$, as introduced in the previous paragraph. Inserting offset to f_{c1} and f_{c2} permits to remove the equilibrium, in term of values of forces, between the two contact forces.

Having the equilibrium between contact forces and equal values of the contact springs stiffness leads the object to be exactly in the middle of the

two fingertips. This works also with the offset introduced via the rest length forces and is valid only in a steady state situation. Changing the values of \mathbf{K}_{c1} and \mathbf{K}_{c2} permits to 'move' the object between the fingertips; in particular the object will be closer to the fingertip with higher stiffness.

From point of view of the object displacement, at the steady state if the joint stiffness $\mathbf{K}_{q1} = \mathbf{K}_{q2}$ for every magnitude of (f_{c1}, f_{c2}) there will be no movements of the central mass. Removing the symmetry between the joint stiffnesses permits to have an asymmetric structure that allows to show the effects of the proposed controller. Doing this permits to the object to move between the action range of the joints. In particular it will move to the direction of the lower joint stiffness.

4.4 Presentation of results

The Simple Gripper is used to analyze the object displacement control effect proposed in the Section 3.3 on a simple example. This goal is achieved in part; further details can be found in Section 5.4. Several simulations were made; for the purpose to show how effective is the control action introduced with the controller proposed, here one is described in details.

The parameters used are in Table 4.1

There are two different control modes, as shown in Section 3.3: with or without the a compensation action. Table 4.2 shows the results obtained in both of them.

Table 4.1: Settings Simple Gripper

Contact Spring left		Contact Spring right	
$K_c = 1000 \text{ N/m}$	$D_c = 40 \text{ Ns/m}$	$K_c = 1500 \text{ N/m}$	$D_c = 40 \text{ Ns/m}$
Fingertip Spring left		Fingertip Spring right	
$K_q = 0.5 \text{ N/m}$	$D_q = 0.2 \text{ Ns/m}$	$K_q = 0.4 \text{ N/m}$	$D_q = 0.2 \text{ Ns/m}$
Left Fingertip Mass = 0.05 Kg		Right Fingertip Mass = 0.05 Kg	
Object mass = 0.25 Kg	$J = \begin{bmatrix} 1 & 0 \\ 0 & 1 \end{bmatrix}$		$G = \begin{bmatrix} 1 & 1 \end{bmatrix}$

Table 4.2: Results compensation action on Simple Gripper

	No Compensation	Compensation
Displacement (m)	0.3526	0.0033

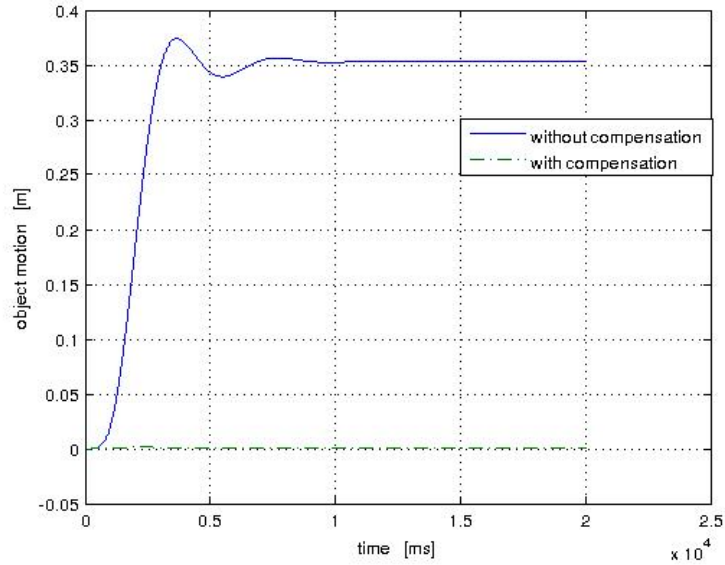


Figure 4.3: Object displacement with and without compensation

The compensation action reduces the displacement of the object of about 100 times. As will be pointed out in the conclusions, the exact zero displace-

ment is not achieved. Hence, these results were considered good enough to validate the constructed block implementing the controller.

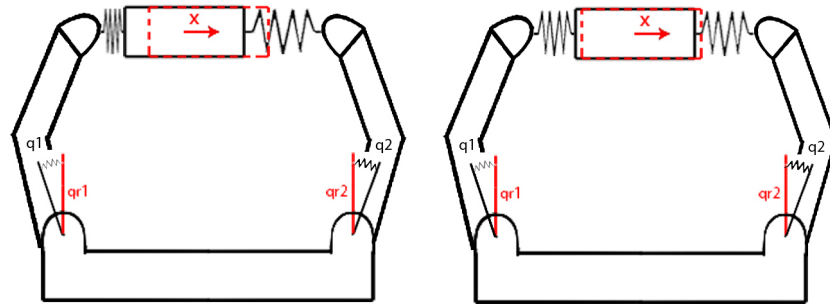


Figure 4.4: Object Displacement control obtained with equations in Section 3.3 - draft caption

In Fig. 4.4 and in Fig. 4.3 is clear the effect of the compensation action. **Note:** The displacements shown in the figure are not representing faithfully the numerical values of the movements and the recover.

Chapter 5

Evaluations

5.1 Simulations

In the previous chapter the controller was tested on a simple example.

In this Chapter more complex examples are taken into account, in particular a realistic model of the robotic hand and the possible inclusion of the postural synergies concept.

The first model to be considered is the Four Fingers problem: the four fingers with three DoFs are considered grasping one object in four points, with a total number of SMD systems equal to 16 (were four of the previous model). It is worth to remember that the SMD modeling the contacts are *isotropic*, i.e. they are spatial system with 3 DoFs behavior.¹

This problem was more complicated compared to the previous one and a fine tuning of the settings was needed to reach a configuration with stable results.

After a successful range of settings was discovered, the analysis moved to the

¹Is possible to see the total number of SMD systems as 16, considering 12 1-D systems and 4 Isotropic systems or 24, splitting the Isotropic contact SMD in 3 single coordinate systems.

third problem: the control model for the real hand. The simulator/controller for the DLR Hand II was already available in the control suite of the RM Institute, hence only an integration was needed.

In the last part of this Chapter is shown how the Postural Synergies concept is inserted in the Simulink model developed for the previous step.

5.1.1 Four Fingers Hand Simulator

The next step was to increase the complexity of the Simple Gripper in order to reach the setting of the multifingered anthropomorphic DLR Hand II [4], hence this is the hardware used in the real experiments.

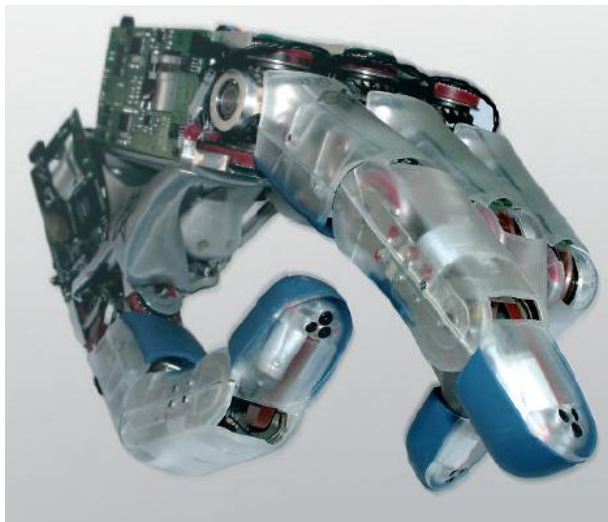


Figure 5.1: DLR Hand II

The device is composed by four identical modular fingers, each of them with three DoFs, for a total number of DoFs equal to 12. Each finger has three joints, that replicates the physiognomy of human finger, and presents the metacarpophalangeal (MCP), the proximal interphalangeal (PIP) and the distal interphalangeal (DIP) joint. Each joint, except the distal ones, is provided with its own motor. The kinematic structure of each finger is bio-

inspired: the MCP joint of each finger has two DoFs, while the PIP joint has a single DoF. The DIP rotation is coupled with the PIP one, with a gear ratio 1:1. Each finger consists of three identical modular parts and has three different type of sensors: each joint is provided with a temperature sensor, a torque sensor and a position sensor.²

To better simulate the real situation, a virtual object is inserted in the model. This virtual object is defined following [17]. It is supposed that the hand grasps an object with its four fingers, the contacts are at the fingertips. From this configuration, the base frame of the virtual object is defined as lying in the middle point of the segment connection the thumb fingertip and the middle fingertip. This segment also defines the X axis, while the Y axis is chosen to be orthogonal to that and placed on the segment connecting the index and the ring fingertip, going from the first to the second. In this way, the plane X-Y is defined; the Z axis is suppose to be orthogonal to this plane, pointing down to the palm of the hand. The base frame defined in shown in Fig. 5.2

Comparing to the previous step, was not possible to use a wide range of settings for the simulation, in order to reach stability, hence a fine tuning of the parameters was needed. In particular, was not possible to reach a difference ratio between \mathbf{K}_{ci} and \mathbf{K}_{qi} of around 1:1000. Only ratios like (0.9-1):(300-400) were reached with the used solver settings, still depending on the values of dampers.

²Notations are considered from [6].

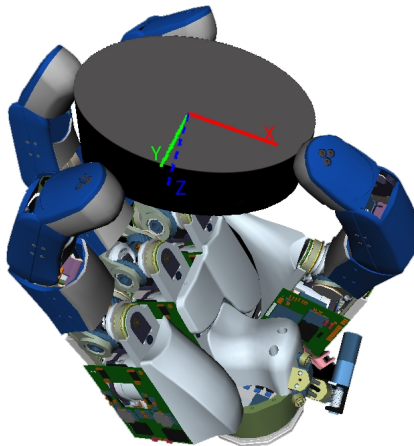


Figure 5.2: DLR Hand II with the object base frame

Table 5.1: Settings Four Fingers

Thumb Stiffness	Index Stiffness	Middle Stiffness	Ring Stiffness
$\mathbf{K}_{q_1} = 9 \text{ N/m}$	$\mathbf{K}_{q_4} = 36 \text{ Ns/m}$	$\mathbf{K}_{q_7} = 36 \text{ N/m}$	$\mathbf{K}_{q_{10}} = 36 \text{ Ns/m}$
$\mathbf{K}_{q_2} = 9 \text{ N/m}$	$\mathbf{K}_{q_5} = 36 \text{ Ns/m}$	$\mathbf{K}_{q_8} = 36 \text{ N/m}$	$\mathbf{K}_{q_{11}} = 36 \text{ Ns/m}$
$\mathbf{K}_{q_3} = 4.5 \text{ N/m}$	$\mathbf{K}_{q_6} = 18 \text{ Ns/m}$	$\mathbf{K}_{q_9} = 18 \text{ N/m}$	$\mathbf{K}_{q_{12}} = 18 \text{ Ns/m}$
Asymmetry between fingers = 4			
Contacts Stiffness		Contacts Damping	
$\mathbf{K}_{c_i} = 350 \text{ N/m}$		$\mathbf{D}_{c_i} = 7.5 \text{ Ns/m}$	
VO Mass	VO Inertia	Interpolator Velocity	
0.15 Kg	$0.03 * \mathbf{I}_{3 \times 3} \text{ Kg} \cdot \text{m}^2$	0.1	
Initial Hand Configuration			
$q_0 = [-0.39 \quad -0.0125 \quad 0.622 \quad -0.2 \quad 0.0629 \quad 0.7422 \quad 0 \quad -0.182 \quad 0.6204 \quad 0.2 \quad 0.2208 \quad 0.6016]^T$			

In the model considering the four fingers hand model an asymmetry between the stiffness of the joints of the fingers was introduced.

This had a practical motivation: as explained also in the Section (4.3) and that can be extended to the four fingers model as well, if in the system is permitted a situation of symmetry between the stiffness of the fingers and of the contacts points, the object will not move, in simulation. To show more displacement a good way was to introduced the asymmetry between the fingers, i.e. to make the thumb more softer than the others (the opposing fingers in this case).

This leads to a bigger movement of the thumb in the squeezing action, seen that the his general stiffness is low.

With general stiffness lower is intended that each stiffness of each joint of the thumb is less than the respective stiffness in the other fingers.

A special analysis was needed on the particular input \mathbf{y} . As seen in Section 3.3, a way to command contact forces is to parametrize them using \mathbf{E} , a basis matrix of the column space of \mathbf{P} , and the vector \mathbf{y} .

$$\lambda_c = \mathbf{E}\mathbf{y}$$

The dimension of \mathbf{E} (n_e) is equal to the dimension of the contact forces vector λ_c (n_f) times the number of independent rows of $\mathbf{P} \in \mathbb{R}^{n_f \times n_e}$, while $\mathbf{y} \in \mathbb{R}^{n_e \times 1}$.

\mathbf{E} changes every time the configuration of the hand changes. In particular the parametrization here defined depends on the Jacobian matrix \mathbf{J} , the grasp matrix \mathbf{G} and the general stiffness matrix \mathbf{K} , i.e. \mathbf{E} can be written as $\mathbf{E}(\mathbf{J}, \mathbf{G}, \mathbf{K})$.

Following what shows above, choosing the vector \mathbf{y} is a non-trivial problem, because it must change as well, considering that the aim is to keep λ_c constant. This constraint is explained considering that λ_c is the reference for the contact forces and it must not change before the system has reached this

value.

Was not possible, for the implementation here describe, to calculate \mathbf{y} dynamically, in order to keep λ_c fixed for each instant of time.

Instead a fixed \mathbf{y} was chosen using the parametrization of the internal contact forces called Virtual Linkage [12].

Following [12], $\mathbf{E}_{vl} \in \mathbb{R}^{n_c \times 6}$ is defined, using the initial position of the fingertips; a $\mathbf{y}_{vl} \in \mathbb{R}^{6 \times 1}$ was choose with this parametrization and we mapped this \mathbf{y}_{vl} onto the \mathbf{E} space in the following

$$\mathbf{y} = \mathbf{E}^+ \mathbf{E}_{vl} \mathbf{y}_{vl}$$

The Virtual Linkage technique was considered because it gives an easy and intuitive way to find a reasonable good \mathbf{y} in order to obtain a consistent group of internal contact forces. What is needed is only to define the magnitude of the forces that are needed along each of the fixed directions ($e_i, i = 1, \dots, 6$), chosen to be the segments connecting all the fingertips.

The chosen \mathbf{y} was considered correct for the purpose of the simulation, also if not the best that can be found.

As for the Simple Gripper, there are two control modes, and in Table 6.1 are shown the results of the application of them.

Table 5.2: Results compensation action on the Four Fingers model

	No Compensation	Compensation
Displacement (m)	0.0165	0.0013

As for the Simple Gripper, the goal of this second step is achieved in part. Is clear that the compensation action in the Four Fingers model is less effective than in the Simple Gripper. We obtain only a 10 times recovery action from the controller proposed in Section 3.3; considering problems shown in

Section 5.4, these results were considered correct for the validation of the controller.

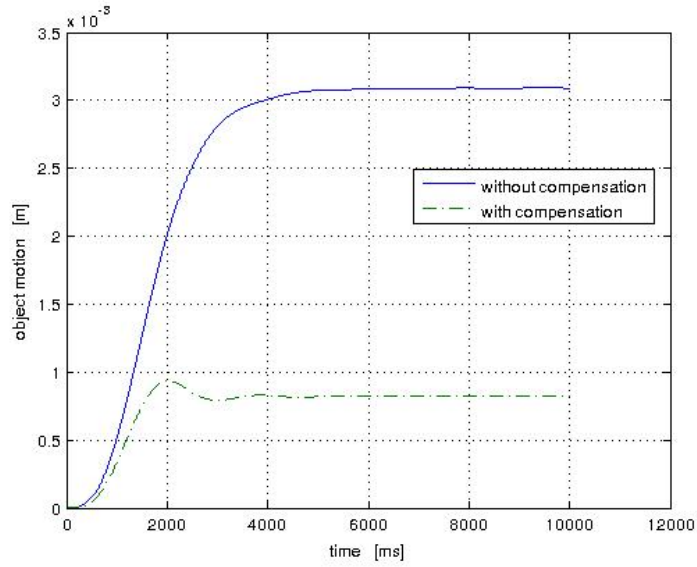


Figure 5.3: Plot object displacement, with and without compensation

In Fig. 5.3, results in terms of module of \mathbf{u} are shown; in Fig. 5.4 results in terms of virtual object displacement are shown, using the 3D Viewer.

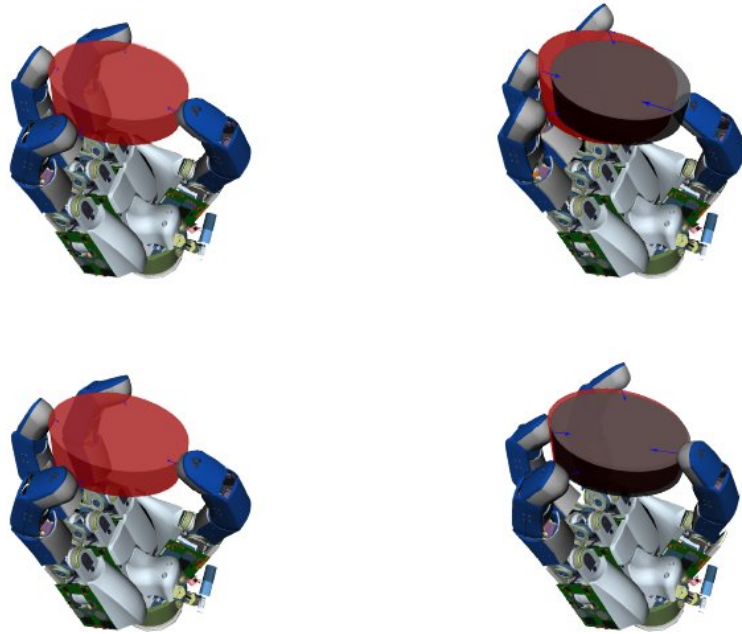


Figure 5.4: 3D Object displacement with and without compensation

A factor of 10 (the compensation effect reduces by 10 times the displacement of the object) was considered a valid result for validating the simulator implemented; hence the next step, the integration with the real hand control model, was implemented.

5.1.2 Hand controller integration

After a successful implementation of the controller was made into a system similar to the real device, the integration step was needed. The idea was to integrate the ODC inside the model controlling the real hand, software already present in the RM Institute control suite. The Simulink model that implements the driving of the DLR Hand II is shown in Fig. 5.5.

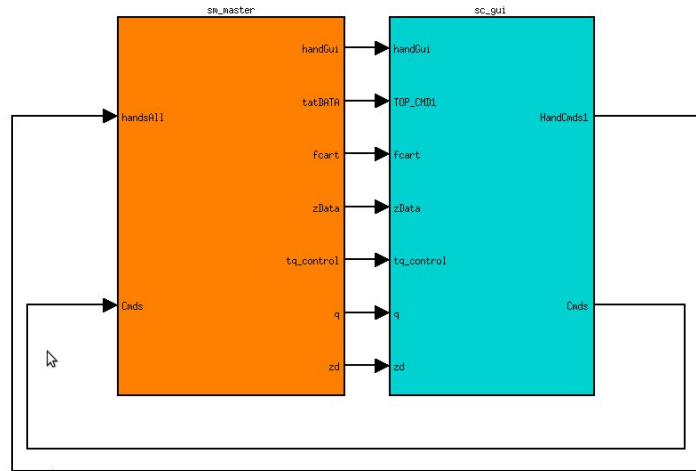


Figure 5.5: Real hand Simulink control model

With this model it is possible to drive the real device, sending PWM signals to the motors of the device, or to run simulations, since inside is included a generic robotic hand model.

First a quick overview on the driving model is made, then a more detailed description of the integration step is given.

The controller is composed of two macro-blocks: **sm_master** e **sc_gui**, respectively the orange block an the cyan block in Fig 5.5. It is worth to remember, there is no real feedback loop between the two block, the signals that **sc_gui** receives from **sm_master** are just showed inside the cyan block, in a GUI.

The two blocks are compiled together but they run on different machines: **sm_master** runs on a QNX machine directly attached to the real device while **sc_gui** runs on a normal machine, with Windows or Linux OS, under Real Time Toolbox of Matlab.

sc_gui has the purpose to provide the user a way to insert inputs for the simulation/control and to give visual outputs of the results.

sm_master contains the controllers and the hand drivers. It demultiples signals coming from **sc_gui** and gives the needed data to the hardware, or to the simulator.

The steps of the integration are :

1. inserting of the Object Displacement Controller (ODC), proposed in Section. 3.3, in the **sm_master** block;
2. include of a input block in **sc_gui** for the ODC;
3. mux of signals from **sc_gui** in order to make them available to **sm_master**, in the form of a signal bus;
4. insertion inside **sc_gui** of a block showing the results of the new controller inserted;

A modification was made respecting the previous model: the calculations of P and V in eq. 3.18 and eq. 3.17 have a sample time 10 times higher than the rest of the system. This means that they are calculated every 10ms instead of 1ms. This change was made to reduce the computational time of the simulations (several times higher than in the previous case) and was considered irrelevant for the evaluation of the correctness of the results.

To judge success of the integration here described a comparison between the results of the previous step and the results of the new model is made. Since there are no relevant differences between the two outputs, the integration was considered correct and the focus moved on the Postural Synergy add.

5.1.3 Postural Synergies control

In the previous section, the ODC controller was successfully implemented for a simple case and for a fully-actuated hand model.

Here the contribution of the Postural Synergies is introduced in the ODC and the step in implementing the SODC (Synergy ODC) is described.

In [1], the authors depicted a way to consider the underactuated approach of the Postural Synergies while decouple the internal forces control and the object movements.

What is shown in the work is here recalled; considering an underactuation approach as the Postural Synergies, it is possible to write variation of the hand joints angles as

$$\delta \mathbf{q} = \mathbf{S} \delta \mathbf{z}$$

where $\mathbf{q} \in \mathbb{R}^{n_q \times 1}$ is the vector of the hand joints angles, $\mathbf{S} \in \mathbb{R}^{n_q \times n_z}$ is the so-called Synergy matrix and $\mathbf{z} \in \mathbb{R}^{n_z \times 1}$ is the input in the synergy space that will be mapped in the joint space, as also shown in the Chapter 2.

In this way, \mathbf{P} and \mathbf{V} are rewritten as

$$\mathbf{V}_S = \mathbf{V} \mathbf{S} \quad , \quad \mathbf{P}_S = \mathbf{P} \mathbf{S},$$

and the desired reference value for \mathbf{z} is

$$\delta \mathbf{z}_c = \delta \mathbf{z}_m + \delta \mathbf{z}_f. \quad (5.1)$$

with

$$\delta \mathbf{z}_f = \mathbf{P}_S^\# \delta \lambda_c \quad , \quad \delta \mathbf{z}_m = -\Gamma_{qc}^S (\Gamma_{uc}^S)^\# V_S \delta \mathbf{z}_f. \quad (5.2)$$

Considering the eq. 5.1, two possible ways to implement the SODC are possible: the first is to obtain $\delta \mathbf{z}_c$ from the control law depicted in the previous

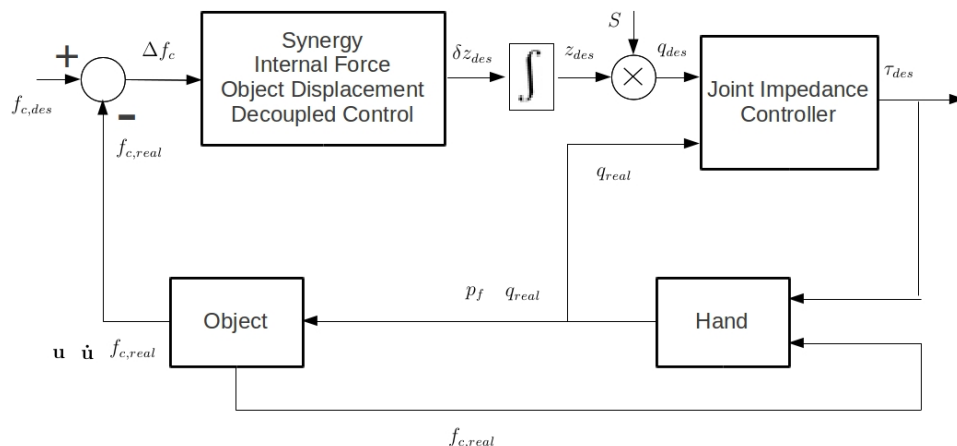


Figure 5.7: Control flow Synergies Integration, joint approach

Unfortunately, for lack of time, was not possible to implement working versions of the SODC. This will be for sure considered in future works, considering that is a fundamental part of the Internal Forces-Object Motion Decoupling technique.

5.1.4 Assumptions

Several assumptions were made concerning the simulations.

First of all, the components of the contact forces that are not direct inside the object are sufficient to satisfy friction constraints. Hence no sliding is allowed.

Then, the contact point is fixed on the fingertip of the finger and cannot move or change during simulations; this leads to have only precision grasps and to have no rolling effects.

External forces or contributions are not considered, first of all, the grav-

ity force. It is assumed that the no sliding constraint and the frictions of the fingertips have a compensation effect against the gravity force. A real compensation contribution can be object of future works, as pointed out in the chapter 7.

The contact model is considered to be Hard Finger (following notation in [8]), so every contact force λ_{c_i} has dimension \mathbb{R}^3 .

Considering 12 joints for the DLR Hand II device and four contact points (one on each fingertip), the dimensions considered in the simulations are the following: $\mathbf{E} \in \mathbb{R}^{12 \times 6}$, $\mathbf{y} \in \mathbb{R}^{6 \times 1}$, $\mathbf{q} \in \mathbb{R}^{12 \times 1}$, $\mathbf{J} \in \mathbb{R}^{12 \times 12}$, $\mathbf{K}_c \in \mathbb{R}^{12 \times 12}$, $\mathbf{K}_q \in \mathbb{R}^{12 \times 12}$, $\mathbf{G} \in \mathbb{R}^{6 \times 12}$. Following this, $\Gamma \in \mathbb{R}^{18 \times 6}$, $\Gamma_{qc} \in \mathbb{R}^{12 \times 6}$, $\Gamma_{uc} \in \mathbb{R}^{18 \times 6}$, $\mathbf{V} \in \mathbb{R}^{12 \times 12}$, $\mathbf{P} \in \mathbb{R}^{12 \times 12}$.

5.2 Experiments

5.2.1 Hardware for experiments

Experiments were carried out at the Institute of Robotics and Mechatronics of the Deutsches Zentrum für Luft- und Raumfahrt (DLR), in Oberpfaffenhofen, near Munich.

The hardware used is composed by:

- the anthropomorphic robotic hand DLR Hand II, described in details in the section 5.1.1;
- a QNX machine, with a Pentium IV processor, 3Ghz, directly connected, via a spacewire port to the device and with a sample time of 1 ms;

- a Windows machine, running a software able to compile the Simulink models for the real time machine and representing the interface and the input GUI for the experiments;
- a soft ball, representing the object that has to be grasped;

5.2.2 Assumptions

Several assumptions were made for the simulations and are depicted in the section 5.1.4.

When considering real settings instead of simulated environments some of these assumptions are not valid anymore.

First of all, the gravity is not considered in the models above described. This can give to the real experiments a contribution that must be taken in account. To overcome this problem, a light soft ball was considered for representing the grasped object; the gravity force related to this object was considered not influent for the performance of the experiments.

However, when more heavy object are considered the gravity contribution cannot be anymore ignored. For this reason, possible way to introduce the gravity force of the grasped object and possible way to compensate this contribution will be analyzed in the future.

The second assumptions that is no more satisfied how the contact is modeled. In the simulations the contact is supposed to be Hard Finger (following [8]), i.e. the contact point is constrained to not move and rotations on the direction not normal to the contact surface are forbidden. It is worth to remember that in the HF contact model the surface for the contact is a point. In real case, the model of the actual contact is much more complex and, in this particular situation, the contact points between the finger and the object

is a surface of the fingertip.

Other assumptions that are not valid anymore in the real experiments are the no-rolling and the no-sliding consideration. When considering a real environment instead of a virtual one, forces like gravity or inertia moments, if not considered inside the model, can give contributions not always predictable to the dynamics of the whole grasp action. The way to avoid that is to set the squeezing forces sufficiently high, in order to let the contact surface to not slide.

For the rolling effect, a way could be to force the contact point on the fingertip to be a single point and not a surface; but having this will be in contrast with the previous sliding-recover effect. At the end, the rolling effect is not recovered but is considered small enough to not contribute in negative way on the results of the experiments.

5.2.3 Modification to the original model

Some changes inside the model were needed when moving from the simulated environment to the reality.

The first modification regards the object motion tracking inside the ODC. The first approach considered was to use a model implementing the equations of the motion of a rigid body, implemented by the RM Institute. This block takes as input the wrench applied to a virtual object (not defined here), his initial frame, his virtual mass and his virtual inertia. From this values and using a Quaternion-based integration, the block is able to give as output the actual frame of the object and his velocity.³

A visual description can be seen in Fig. 5.8.

³For details about Quaternion, refer to [19].



Figure 5.8: Object Tracking Block

The classical approach is to use the velocity of the fingertips and the Grasp matrix following the first of the two equations in (3.8), $\nu_c = \mathbf{G}^T \nu_u$, to extrapolate the velocity of the object. On this velocity a Quaternion-based integration is made (like in the previous method) and the actual frame related to the object is found. From the frame is then retrieve the actual position of the object.

Also if this is still a numerical tracking of the grasped object, and is not based on real measure of the position, it was considered a good and quick way to find the actual position.

The second modification that was needed regards the calculation of the actual contact forces. In the original model, the contacts are modeled like a system provided with a spring and a damper attached to the fingertip and to contact point on the object. This follows directly from the assumption that the contact point on the fingertip and on the object could also not be the same and that the position of the fingertip can also enter the object. Obviously in the real case this way to model the contact has no sense anymore.

When considering the real device, is possible to use the torque on the joints to have an estimation of the contact forces at the fingertips, as the eq. (3.11) shows.

An approach of this kind was used in the experiments model taken in account.

5.2.4 Setup

The initial configuration for the simulations was a situation of the grasp of an object without contributions from the contact forces.

Hence, to perform in the same way as in the simulations, a research of a correct initial configuration for the grasping experiments was needed.

Once this configuration was achieved, was however possible to see a phenomenon of hysteresis on the torque sensors that was directly translated to the contact forces values. This soft hysteresis leads to having a non zero difference between the desired contact forces and the actual contact forces also in case of zero input. For this reason a "Threshold control" was introduced to filter this phenomenon and permits to have the expected results in case of zero input.

In the following box is shown the code of the "Threshold control"

```
function y = fcn( u, T )  
  
y = zeros(length(u),1);  
  
for i = 1:length(u)  
    if abs(u(i)) < T  
        y(i) = 0;  
    else  
        y(i) = u(i);  
    end  
end
```

The introduction of this control on the desired force variation made possible the correct initialization of the settings.

5.2.5 Settings

The first step of the experiments was, as pointed out before, to set an initial configuration of the joints that was not giving contributions on the contact forces measurements.

The following steps were then performed:

- activating a Joint Impedance Controller to set up a safe base for the experiments;
- the control was switched on the ODC, while keeping the hand still off;
- the hand was switched on and it was driven by references given by the ODC.

With safe base is intended a situation well know and without presence of errors (in calculation as in measurements of sensors).

This situation is considered safe due to the large experience and background hold and given from previous works on the Joint Impedance Controller, made by the team of the DLR.

The idea that lies under this steps is to find before a safe position for the hand, in sense of no errors and no unexpected behaviors, then to switch to the ODC (the experimental part) and to evaluate that.

5.2.6 Performance

Unfortunately, the behavior of the ODC was not the one expected. Was not possible to obtain the results as in the simulations; this is probably amenable to the not correct parametrization of the internal forces \mathbf{y} .

It was seen that commanding the same \mathbf{y} as in the simulations was leading to an opening of the hand, that is the opposite of the squeeze that was expected. Even changing the sign to the input, that would lead to a squeeze of

the grasped object, didn't bring the expected result.

Was then concluded that some interpretation problems on \mathbf{y} were presents, but the resolution of them was considered out of the scope given to this work.

The integration time was subject to time constraints and within this time period it was not possible to make it work.

5.3 Problems solved

The main problem that were solved is related to the parametrization matrix for the internal forces \mathbf{E} . As already described in the Section 3.3, \mathbf{E} is a basis of the matrix \mathbf{P} and in the Simulink model is calculated using the Singular Value Decomposition (SVD) technique. This technique has a problem while the singular values that come out as results are close to the axis defined with SVD. In this case, is possible that the same value is given in one calculation with positive sign and in another calculation with negative sign.

The problem leads to the eventuality that in a simulation with thousands of calculation of SVD, like in the case taken in account, the values composing the matrix \mathbf{E} change sign from one time slot to the other, with a complete change in the meaning of the equation $\lambda_c = \mathbf{E}y$.

In this case, the reference forces are changing sign and orientation every iteration and this makes impossible to the torque controller to follow reach the references.

A solution found for this problem was to block these changes, making impossible to switch sign from one iteration to the next if their value doesn't change in module.

Here the code of the fix is shown:

```
function newE = comp(E, Eold)
    [a,b] = size(E);
    newE = zeros(a,b);

    for i=1:b
        if (change_sign(E(:,i),Eold(:,i)) == 1)
            %sign changed
            newE(:,i) = Eold(:,i);
        else
            %sing unchanged
            newE(:,i) = E(:,i);
        end
    end

function fl = change_sign(a,b)

    aux = 0;
    for j=1:length(a)
        if ( (sign(a(j)) * sign(b(j))) < 0 )
            if (aux == 0 )
                aux = 1;
            end
        end
    end
    fl = aux;
```

In this way, a correction of the \mathbf{E} matrix was possible just giving as input to the function the current value of \mathbf{E} and the value at the step before.

5.4 Problems unsolved

In this section, the unsolved problems discovered during the work are depicted. For some of them, possible solutions are given.

5.4.1 Cascaded control loops

Due to the formulation of the ODC and of the implementation here presented, it was not possible to avoid the presence of a cascaded force control loop. In the Fig 5.9 is shown this concept.

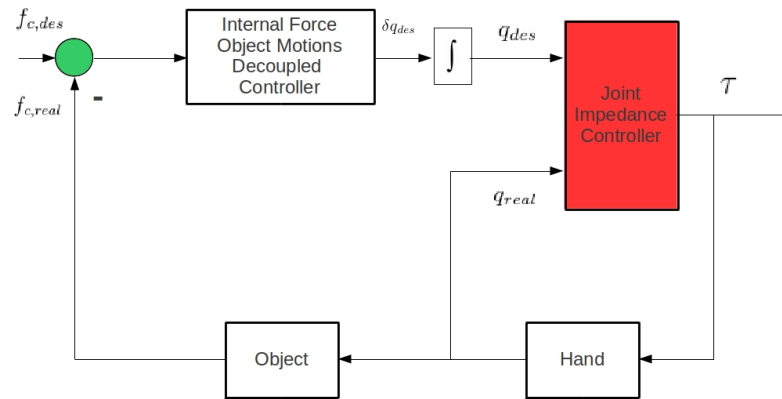


Figure 5.9: Cascaded control loops

The first loop is closed in the red block, where a difference between the desired joints positions and the real joints positions, that arrive from the real hand or from the model of it, is made. The second loop is closed in the green block, that is difference between the desired internal forces and the forces that there are really on the contact.

In the control theory, is known that in situations like this, the inner loop gain must be faster than the outer loop gain. The difference in the 'velocity' of calculation is necessary for the outer loop to calculate correctly results; if the inner loop is faster, is possible that the inner results change too fast for the outer loop to use them in a significant way and the whole output of the system is not correct.

In order to simulate a consistent real situation, a ratio of $\sim 1000:1$ between contact stiffness and joint stiffness was needed. Hence this ideal setting

was not reachable for the simulations here considered because to guarantee stability was not possible to set a ratio higher than $\sim 100:1$. This led to $\mathbf{K}_{c_i}:\mathbf{K}_{q_i} = (300-350):(0.5-1)$ N/m, while in the ideal case would be $\mathbf{K}_{c_i}:\mathbf{K}_{q_i} = (1000-2000):(0.5-1)$ N/m.

A solution to this problem is still under study, as is pointed out in the Chapter 7.

The setting of the solver for the simulations was considering the ODE1 differential equations solver, provided by Matlab and implementing the first-order Euler method.

The sample time for the simulations was 1 ms.

5.4.2 Quasi-static analysis vs. dynamical simulation

The problem depicted before was concerning differences in modeling contact forces.

A difference can be found between the work presented in [1] and the real implementation of the ODC : what proposed in the work of Prattichizzo-Malvezzi is a quasi-static analysis of the decoupling of internal forces and object displacement. From an equilibrium point, the system is considered after one infinitesimal instant of time and the controller is validated. In this real implementation of the controller, dynamic simulations and experiments are performed. The equations given in [1] are valid in a static setting; hence, they still hold in dynamic conditions if the system is asymptotically stable and the superimposed variations are small (otherwise the linear approximation is no more satisfied) and constant or slowly variable (slow with respect to system time constants).

Having a slow increase of the input permits to have difference between the desired contact forces and the actual contact forces that can be considered

small enough to not invalidate the controller.

Hence, this is one of the biggest doubt that lies on the results of every simulators performed and on the experiments, since in the linear case worked better.

5.4.3 Time dependencies

The last unsolved problem that was discovered is related to the commanded internal forces and their supposed dependencies on time. As already mentioned before, the controllable internal forces can be written using \mathbf{E} , a basis matrix of the column space of \mathbf{P} , and \mathbf{y} as

$$\delta\lambda_c = \mathbf{E}\mathbf{y}.$$

What is needed for the controller is a reference for the desired internal forces $\lambda_{c,r}$ that represents the variation with the respect to the equilibrium configuration.

\mathbf{E} is a function of \mathbf{J} , \mathbf{G} , \mathbf{K}_q and \mathbf{K}_c . The Jacobian of the manipulator and the grasp matrix are depending on the actual configuration of the joints, so it is clear that also \mathbf{E} will depend on the joint state \mathbf{q} .

Having a fixed \mathbf{y}_r and a changing \mathbf{E} shows that \mathbf{y} must change as \mathbf{E} and the product must remain constant for each instant of time.

The two matrices \mathbf{J} and \mathbf{G} are calculated inside the ODC while the vector \mathbf{y} is given as input outside the controller. To permit to the right side of (5.4.3) to be constant is needed that \mathbf{y} is evaluated inside the controller and is based on changes of \mathbf{q} as \mathbf{E} . This implementation was out of the scope of this work and it remains an open issue.

5.5 Software used

The software used for the implementation of the models and for their validation is Mathworks Matlab R2007b, using the environment Simulink, under the distribution of Linux OpenSUSE.

Chapter 6

Discussion

In this chapter are discussed the results obtained in this work.

To resume briefly, four steps were made in this Thesis:

- implementation of a simple example, Simple Gripper, with the purpose to validate the proposed controller;
- extension of this example considering a more complex case, the four fingers model of the DLR Hand II;
- integration of the result of the previous step inside the model driving the real device;
- explaining how to integrate the Postural Synergies in the proposed controller and how to use the Synergy-based Impedance Controller;
- performing of experiments with the purpose to validate the proposed controller also in a real environment.

The analysis started from a simple example, concerning two one-joint fingers squeezing a mass in 1-D. Results on this step are provided in the relative chapter.

As already pointed out, this example was used to validate the Simulink block

that implements the ODC.

The validation has been successful and the block implemented in this step is used later in the others. Considering the difference between the quasi-static analysis of [1] and the dynamic evolution of the system that belongs to simulations and experiments, around 100 times of reduction in the displacement of the object was considered good for proceeding in the others steps.

The next step was to complicate the problem of the Simple Gripper and to consider four fingers, each provided with four joints, three of them controllable, because two strictly coupled; the whole environment is still a fine grasp of an object. The system references moved from 1-D to 3-D and in the model a Joint Impedance Controller was needed. The model, at the time of this step, contained the Internal Forces-Object Motions Decoupling Controller, the Joint Impedance Controller, the hand dynamics simulator and the object simulator block. The structure of the Simulink model can be seen in Fig. 6.2

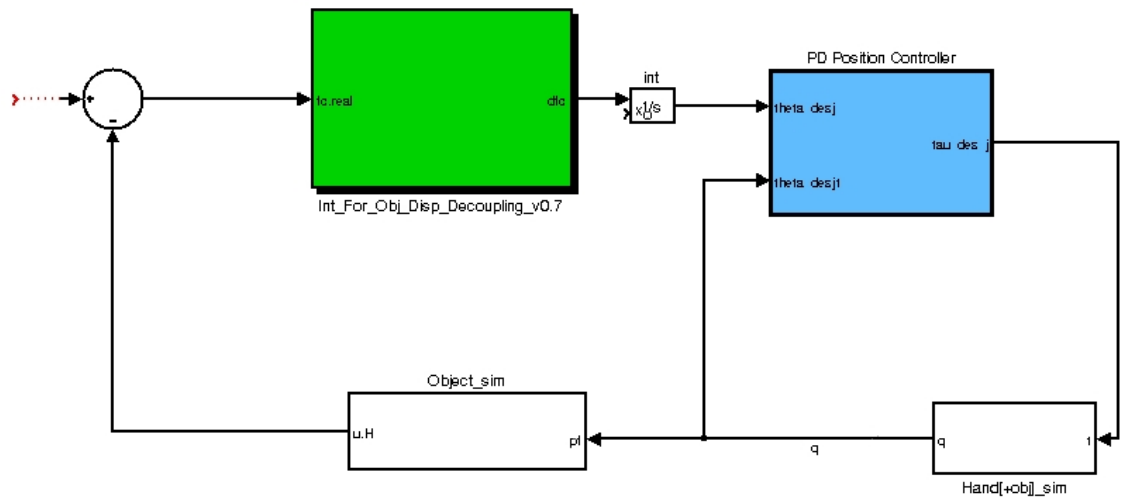


Figure 6.1: General four fingers model structure

As is possible to see in Fig. 5.3 and in Tab 6.1, a recovering of around 10

times in the object displacement was reached. This was judged sufficiently correct to proceed in the following steps.

The main reason why, in the opinion of the author, is not possible to recover completely the displacement of the simulate object has been searched in the difference between the quasi-static analysis and the dynamic simulation made here. Anyway, considering the good results obtained and the relatively new approach to the problem, a deeper analysis was not performed; this will be a subject that can be considered in the future works.

Results from the third step, the inclusion of the four fingers simulator inside the real hand control block, are given here.

Table 6.1: Results compensation action on the third step

	No Compensation	Compensation
Displacement (m)	0.01648	0.001260

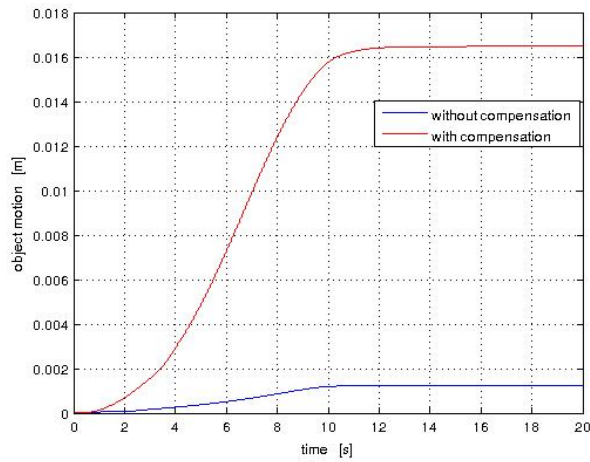


Figure 6.2: Plot results on the third step

As is clear, there are no relevant differences between these results and the results obtained with the four fingers simulator.

Before trying the proposed controller with a real setup, the integration of the Postural Synergies in the ODC was considered, strictly following [1]. Unfortunately was not possible to implement a working version of that, in the time that was given for this work. This can be a possible future work.

About the experiments, as already said in the Chapter 5, it was not possible to obtain results with them. The real performing of the proposed controller has to be considered not working, at least at the point where this work is arrived.

It is worth to remember that an important problem on the setting of the parametrization of the internal forces was found during the the real experiments; perhaps solving this can lead to a working behavior of the ODC. In the time that was dedicated to this work, was not possible to find a solution to this problem.

Chapter 7

Conclusions

7.1 Conclusions

In this work the major objective was to develop and to analyze in dynamic condition the Internal Forces-Object Motions Decoupling controller. It focuses on the internal forces variation while avoiding movements of the grasped object.

A deep analysis of the proposed controller was made and a dynamical simulator was developed, considering compliant robotic manipulator grasping an object. The built simulator was then improved taking in account the multi-fingered robotic hand DLR Hand II. A four-finger grasp was considered and a dynamic evolution of this, with internal forces variation, was studied. The resulting successful implementation was experimented on a real version of the DLR Hand II and assumptions made for the virtual environment were removed.

Considering what shown in the Chapter 6, is possible to say that the implementation of the controller proposed was not completely a success. Moving from a quasi-static analysis to a dynamic analysis may have introduced un-

foreseen problems and considering this the obtained results are considered from the author a proof valid enough for the validation of the ODC.

7.1.1 Future Works

Several future works can be thought considering the work here described.

First of all, the integration of the Postural Synergies in the ODC if the main focus of future works related to what done here. As already said, was not possible for lack of time to implement the SODC in a working version; comparing the results from the previous versions of the ODC with the new approach will be for sure an interesting topic that can be analyzed.

Second, including contributions of external forces, like the gravity, can be a key topic. The implemented controller doesn't consider contributions that are not coming from the grasping activity, so will be possible to include in the equations and in the control law possible external wrenches. This topic is strongly important while looking at the experiments that is possible to perform with the real robotic device because this is the assumption that is more difficult to overcome, in case of real environment.

Another possible extension of this work is to apply to five fingers robotic devices the implemented controller, in order to have a comparison 1:1 between the Prattichizzo et al. work and what is done here. Having the same considered number of fingers as in the human hand opens the possibility of more consistent comparisons.

A fourth inclusion that can be considered is about pre-load forces. In the actual implementation commanded forces start from a initial value equal to

0; while grasping an object having contact forces equal to 0 can be possible only in case of high transversal stiffness in the fingertips. Hence, a complete covering of this problem can be made in the future, concerning variations of internal forces that don't start from 0.

A situation of cascaded control loop was needed to implement correctly the proposed controller. This led to some limitations about the settings, in particular on the ratio between \mathbf{K}_{c_i} and \mathbf{K}_{c_i} . A solution to this problem can be an important future work and can permit to simulate more consistent real environments.

A last but not least analysis can be done on the computation of a proper \mathbf{y} for controlling the desired internal forces. This was the main problem encountered in the experimental part of the work and it must be overcome to have the possibility to achieve real data for the controllers here introduced. In addition, a way to calculate dynamically \mathbf{y} can be implemented in the Simple Gripper and in the Four Fingers Hand example.

Bibliography

- [1] M. Malvezzi and D. Prattichizzo. Internal force control with no object motion in compliant robotic grasps. In IEEE/RSJ International Conference on Intelligent Robots and Systems, 2011.
- [2] M. Santello, M. Flanders, and J.F. Soechting. Postural hand synergies for tool use. *The Journal of Neuroscience*, 18(23):10105-10115, December 1998.
- [3] Thomas Wimböck, Benjamin Jahn and Gerd Hirzinger. Synergy Level Impedance Control for Multifingered Hands. In IEEE/RSJ International Conference on Intelligent Robots and Systems, 2011.
- [4] J. Butterfaß, M. Grebenstein, H. Liu, and G. Hirzinge. DLR-Hand II: Next generation of a dextrous robot hand. In IEEE International Conference on Robotics and Automation, 2001.
- [5] G. Cannata, M. Maggiali, G. Metta and G. Sandini. An Embedded Artificial Skin for Humanoid Robots. In IEEE International Conference on Multisensor Fusion and Integration for Intelligent Systems, 2008.
- [6] S. Mulatto, A. Formaglio, M. Malvezzi, D. Prattichizzo. Animating a synergy-based deformable hand avatar for haptic grasping. In *Lecture Notes in Computer Science*, 2010, Volume 6192/2010, 203-210.

-
- [7] R. Murray, Z. Li, and S. Sastry, *A Mathematical Introduction to Robotic Manipulation*. CRC Press, 1994.
- [8] D. Prattichizzo and J. Trinkle. Grasping, pages 671-700. Springer, 2008.
- [9] D. Prattichizzo and A. Bicchi. Dynamic analysis of mobility and graspability of general manipulation systems. *IEEE Trans. on Robotics and Automation*, 14(2):241-258, April 1998.
- [10] D. Prattichizzo and A. Bicchi. Consistent specification of manipulation tasks for defective mechanical systems. *ASME Journal Dynamic Systems, Measurement, and Control*, 119:767-777, December 1997.
- [11] D. Prattichizzo and A. Bicchi. Consistent Task Specification for Manipulation Systems With General Kinematics. *Journal of Dynamic Systems, Measurement, and Control*, 119(4):760, 1997.
- [12] D. Williams, O. Khatib. The Virtual Linkage: A Model for Internal Forces in Multi-Grasp Manipulation. *ICRA (1) 1993*: 1025-1030.
- [13] A. Wing, P. Haggard, J.R. Flanagan. *Hand and Brain: Neurophysiology and Psychology of Hand Movements*. Academic Press Inc 1998.
- [14] L. Birglen, C. Gosselin, T. Laliberté. *Underactuated robotic hands*. Springer, 2008.
- [15] D. Prattichizzo, M. Malvezzi, A. Bicchi. On motion and force controllability of grasping hands with postural synergies. *Robotics: Science and Systems*, 2010.
- [16] M. Ciocarlie, C. Goldfeder, P. Allen, *Dexterous Grasping via Eigen-grasps: A Low-dimensional Approach to a High-complexity Problem*. *Robotics: Science and Systems*, 2007.

-
- [17] T. Wimböck, C. Ott, G. Hirzinger. Passivity-based Object-Level Impedance Control for a Multifingered Hand. IROS 2006
- [18] M. Grebenstein, A. Albu-Schäffer, T. Bahls, M. Chalon, O. Eiberger, W. Friedl, R. Gruber, S. Haddadin, U. Hagn, R. Haslinger, H. Höppner, S. Jörg, M. Nickl, A. Nothhelfer, F. Petit, J. Reill, N. Seitz, T. Wimböck, S. Wolf, T. Wusthoff, and G. Hirzinger. The DLR Hand Arm System. ICRA 2011
- [19] F. Caccavale, B. Siciliano, L. Villani. The Role of Euler Parameters in Robot Control. Asian Journal of Control, Vol. 1, No. 1, pp. 25-34, March 1999